PHYSICAL REVIEW B VOLUME 56, NUMBER 12 15 SEPTEMBER 1997-II

Carrier quantum confinement in self-ordered $Al_xGa_{1-x}As$ V-groove quantum wells

E. Martinet, A. Gustafsson, G. Biasiol, F. Reinhardt, and E. Kapon
Département de Physique, Ecole Polytechnique Fédérale de Lausanne, CH-1015 Lausanne, Switzerland

K. Leifer
Centre Interdépartemental de Microscopie Electronique, Ecole Polytechnique Fédérale de Lausanne, CH-1015 Lausanne, Switzerland

(Received 16 July 1997)

Observation of quantum confined states and optical anisotropy of the interband absorption in self-ordered $Al_xGa_{1-x}As$ vertical quantum wells (VQW's) grown on V-grooved substrates is reported. The variation in Al composition across the VQW's was determined by parallel electron energy-loss spectroscopy. It was then employed to calculate the eigenstates of the confined carriers in these structures, with valence-band mixing included using a 4×4 $\mathbf{k}\cdot\mathbf{p}$ Luttinger model. Polarized photoluminescence excitation spectra of the structure show features attributed to transitions between electron and heavy-hole or light-hole confined eigenstates, with measured energies in good agreement with the calculated ones. Polarization anisotropy associated with confined electrons and holes is evidenced by the measured spectra and explained by valence-band mixing in the (011) self-ordered quantum well. [S0163-1829(97)51936-9]

A method for preparing quasi-two-dimensional quantum well (QW) heterostructures, namely, via self-ordering of $Al_xGa_{1-x}As$ grown by organometallic chemical vapor deposition (OMCVD) on V-grooved GaAs substrates, has been investigated.[1,2] These structures consist of Ga-rich, thin (<20 nm) ''vertical'' regions formed at the center of a [011] oriented groove, surrounded by higher band gap $Al_xGa_{1-x}As$ barriers. The effect of the growth conditions (temperature and reactor pressure) and Al nominal composition of the $Al_xGa_{1-x}As$ layer on the Ga segregation—and hence the vertical quantum well (VQW) potential depth and width—has been studied.[2–4] Low-pressure (LP) (20 mbars) growth was demonstrated to yield extremely narrow (a few nm wide) multiple-VQW's with well-defined features.[4] The distribution of Al composition across the VQW was evidenced by atomic force microscopy (AFM) with a limited (a few nm) spatial resolution.[4] The optical properties of such VQW structures have been investigated by low-temperature photoluminescence (PL) (Ref. 2) and cathodoluminescence (CL) techniques.[3,5] Polarization anisotropy in the PL spectra of a VQW was observed and was explained by the polarization selection rules for the interband transitions due to confinement effects along the [011] direction.[2] More recently, lasing in laser diodes incorporating VQW structures was demonstrated with output beams polarized in the VQW planes, and was explained by the anisotropy in the laser gain due to lateral confinement.[6] Polarization anisotropy was also observed in the infrared absorption spectra in *n*-doped VQW structures and was attributed to the polarization selection rules for the electronic intersubband transitions in the conduction band.[7] The role of VQW's in promoting the carrier capture into quantum wires (QWR's) embedded in the VQW structure was also discussed.[1,5,8] The variation of VQW radiative lifetimes measured by time-resolved PL as a function of temperature was reported as an indirect signature of two-dimensional confinement in the VQW.[9]

In this paper, we report on direct evidence of lateral quantum confinement in VQW structures by PL excitation (PLE) spectroscopy. The Al composition across the VQW was independently determined with high resolution using parallel electron energy-loss spectroscopy (PEELS) in a transmission electron microscope. The interband transition energies in the VQW, deduced from PLE spectra, are in good agreement with the calculated transition energies based on the measured Al composition profile and a 4×4 $\mathbf{k}\cdot\mathbf{p}$ Luttinger model. Polarization anisotropy in the PLE spectra is explained by two-dimensional lateral confinement and mixing in the valence band of the (011) self-ordered QW.

The structures investigated were grown on a semi-insulating (100) GaAs substrate patterned with 3 μm pitch, 1.5-μm-deep V-groove gratings oriented along the [011] crystal direction. The growth was performed at low pressure (LP, 20 mbars) in a horizontal OMCVD reactor, at a substrate temperature of 700 °C.[4] Figure 1(a) is a schematic illustration of a typical sample, consisting of a 500 nm $Al_xGa_{1-x}As$ core layer, sandwiched between two

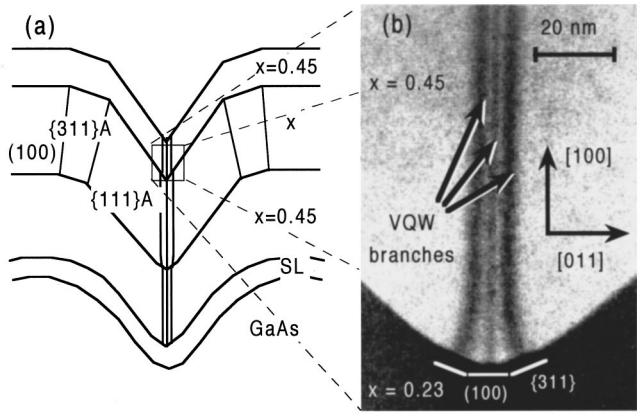

FIG. 1. (a) Schematic cross section of a VQW heterostructure. (b) Dark field TEM micrograph showing a cross-sectional view of a typical self-ordered VQW region in $Al_{0.45}Ga_{0.55}As$ on a self-limiting $Al_xGa_{1-x}As$ ($x_{nom}=0.23$) layer grown on a V-grooved GaAs substrate.

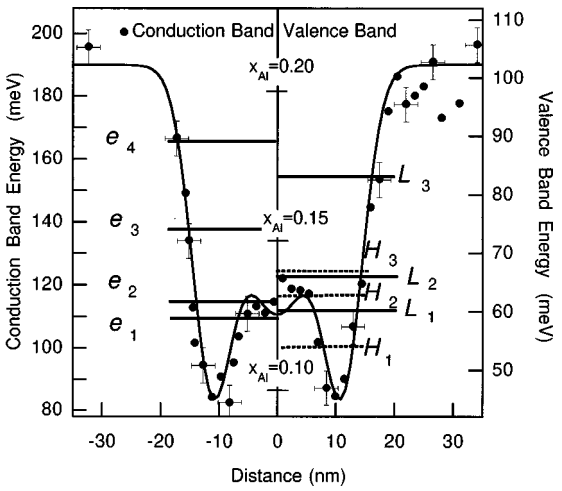

FIG. 2. VQW Al profile obtained from parallel-EELS measurements (circles). Triple-Gaussian fit of the VQW potential profile and calculated subband energies for electrons (e_i), heavy holelike (H_i) and light holelike (L_i), are also shown ($x_{\mathrm{nom}}=0.21$).

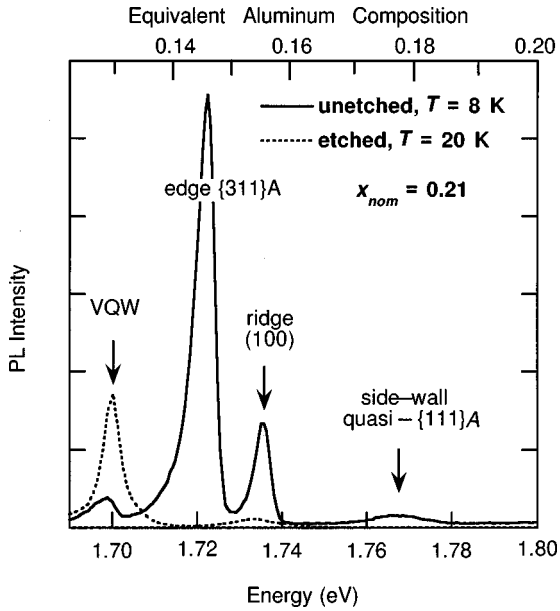

FIG. 3. Photoluminescence spectra of the VQW sample with background Al composition $x_{\mathrm{nom}}=0.21$, measured at $T=8$ K on an unetched sample (full line), and at $T=20$ K for a sample where the $\{311\}A$ edge and (100) ridge regions were removed by selective etching (dashed line).

$Al_{0.45}Ga_{0.55}As$ layers (400 nm at the bottom and 100 nm at the top). We grew different samples with the nominal x in the core (x_{nom}) ranging from 0.09 to 0.45. A short period (1.5/1.25 nm) $GaAs/Al_{0.45}Ga_{0.55}As$ superlattice (SL) was used as a buffer layer. x_{nom} in the core was measured by x-ray diffraction on a reference sample grown simultaneously on a planar (100) GaAs substrate. Figure 1(b) is a cross-sectional dark field transmission electron microscope (TEM) image of the upper interface of an $Al_xGa_{1-x}As/Al_{0.45}Ga_{0.55}As$ V-groove structure with $x_{\mathrm{nom}}=0.23$. It shows a triple-well VQW structure made of narrow (a few nm wide) well-defined branches in the cladding ($x=0.45$) layers. Three branches that are similar are observed in the core region of interest (with x_{nom}).[4] The side and central branches are seeded by $\{311\}A$ and (100) self-limiting facets on the $Al_{0.24}Ga_{0.76}As$ layer at the bottom of the groove. Self-limiting growth of the VQW in the $Al_xGa_{1-x}As$ layer is achieved within less than 20 nm, followed by a uniform growth across the layer. Good uniformity of the VQW over a measured range of several microns along the [011] crystal direction was also observed in the top view TEM images.

Figure 2 is a plot of the Al composition distribution across the VQW in the core layer, in a sample with $x_{\mathrm{nom}}=0.21$, showing two distinct VQW branches separated by 17 nm and a barely resolved center branch. The Al composition profile was measured by PEELS, and the data were deconvolved to take into account the finite spatial resolution (5 nm) resulting from the finite size of the focused beam.[10] The measurement was optimized for absolute Al composition accuracy, yielding a 0.02 resolution in the absolute Al mole fraction and 0.01 for the relative Al mole fractions between two regions of the sample.[10] The quasi-$\{111\}A$ barrier composition at the edge of the VQW layer and at the bottom of the VQW were measured to be $x_{\mathrm{PEELS}}^{\mathrm{barrier}}=0.21\pm0.02$, and $x_{\mathrm{PEELS}}^{\mathrm{VQW}}=0.10\pm0.02$ at the bottom of the VQW, respectively. The maximum segregation in the VQW is $\Delta x_{\mathrm{PEELS}}^{\mathrm{VQW}}=0.11\pm0.01$. The profile of the three branches of the VQW is well described by a triple-Gaussian fit (solid line in Fig. 2).

Figure 3 (solid line) shows the PL spectrum of the VQW sample with $x_{\mathrm{nom}}=0.21$, measured at $T=8$ K with an argon ion laser beam (488 nm), at a power density ≈ 1 W/cm^2. The PL spectrum is dominated by luminescence at 1.723 eV. The lowest energy peak at 1.698 eV is identified as the emission from the VQW; it becomes the dominant PL peak in a selectively etched sample where the $\{311\}A$ and (100) regions were removed[1] (dotted line spectrum in Fig. 3). The emission at 1.723 eV originates from the $\{311\}A$ edge region between the top (100) ridge and the quasi-$\{111\}A$ sidewalls, the emission at 1.736 eV originates from the narrow (100) ridge region, and the one at 1.767 eV is due to recombination at the quasi-$\{111\}A$ sidewalls (see Fig. 1). These peak assignments were confirmed by low-temperature, cross-sectional CL imaging of the emission wavelengths. The linewidth of the VQW transition is 6 meV full width at half maximum, consistent with the good structural uniformity of the VQW measured along the [011] and the [100] directions. At temperatures above 80 K, the VQW dominates the PL spectra even in the unetched samples, due to the efficient, thermally activated carrier transfer from the $\{311\}A$ regions into the VQW.[11]

Low-temperature ($T=8$ K) PLE spectra of the VQW sample detected at the VQW transition line (1.698 eV) are displayed in Fig. 4. The spectra were measured using a tunable Ti:Sapphire laser directed normal to the (100) substrate plane, with the pump beam linearly polarized parallel ($\parallel$) or perpendicular ($\perp$) to the VQW plane. Contribution of absorption in the $\{311\}A$ edge facets in the VQW luminescence was identified by careful measurements of the PLE spectra as a function of sample temperature, and comparison with the samples where the $\{311\}A$ were etched out. It is concluded that the PLE signal detected at the VQW emission line uniquely reflects the joint density of states (DOS) for interband transitions in the VQW. Several features corresponding

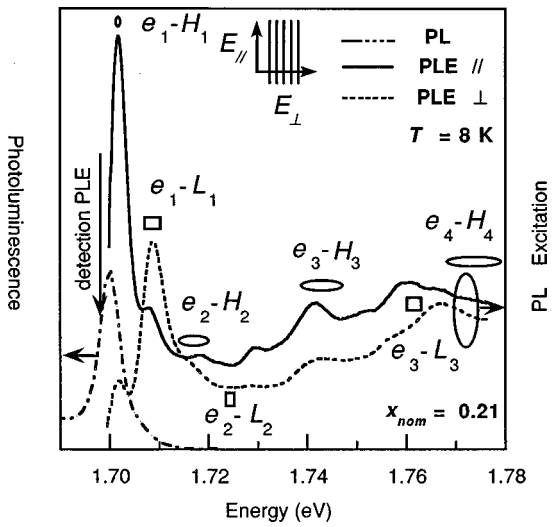

FIG. 4. PL and polarized PL-excitation spectra of the VQW of Fig. 2, with background Al composition $x_{\mathrm{nom}}=0.21$. Symbols indicate various calculated e-H (open ovals) and e-L (open squares) transition energies.

to transitions between quantum confined eigenstates can be observed in the PLE spectra. The peaked lineshapes suggest the excitonic nature of the transitions. The measured Stokes shift of ~ 4 meV is consistent with the narrow PL linewidth.

We used a simple model to calculate the energy levels of the confined states in the VQW, neglecting Coulomb correlation effects. The triple-Gaussian fit to the measured Al composition profile (Fig. 2) was used to model the confinement by employing the well-established dependence of the direct gap of $Al_xGa_{1-x}As$ on x,[12] and assuming 65/35 conduction to the valence-band offset ratio. The PEELS measurements yield a 160 ± 15 meV potential energy depth for the VQW, and a 1.660 ± 0.030 eV band gap energy at the bottom of the VQW. Due to low symmetry in the (011) direction, heavy- (hh$=|3/2,\pm 3/2\rangle$) and light-hole (lh $=|3/2,\pm 1/2\rangle$) states are mixed even at the Brillouin zone center (BZC). Valence-band mixing was taken into account by diagonalizing the 4×4 $\mathbf{k}\cdot\mathbf{p}$ Luttinger Hamiltonian using a $|J,M_J\rangle$ basis with quantization along the [011] direction, resulting in heavy- (H) and light- (L) holelike states.[13] The eigenenergies for electrons (e_j) and holes (H_j,L_j) were solved numerically for the envelope states, with the effective mass for electrons and holes (H,L) obtained from the Luttinger parameters.[14] The calculated levels are displayed in Fig. 2.

Figure 4 shows the position of the calculated first e_j-H_j (open ovals) and e_j-L_j (open rectangles) transition energies together with the PLE spectra, after adjustment of the calculated energy of the e_1-H_1 to the measured peak of lowest energy. This difference between the measured (1.703 eV) and calculated (1.693 ± 0.030 eV) energy for the e_1-H_1 transition is within the uncertainty in the potential energy at the bottom of the VQW, even after allowing for excitonic binding energy in the measured transition energy. The error in the calculated energies (represented by the length of the symbols in Fig. 4) results both from the inaccuracy in the potential profile (measured by PEELS) and that in the γ Luttinger parameters. Good agreement is obtained between the excitonic peaks and step edges of the measured DOS and the calculated first e-H and e-L transition energies. The 6.5 ± 1.5 meV calculated energy difference between e_1-H_1 and e_1-L_1 is in excellent agreement with the measured value (7 ± 1 meV). The fact that the PLE spectrum at higher transition energies exhibits less well-defined excitonic features could be explained by alloy broadening in the $Al_xGa_{1-x}As$ VQW and by the presence of numerous L- and H-hole states, whose energies are very sensitive to details in the potential profile.

Comparison of the two polarized spectra in Fig. 4 reveals strong polarization anisotropy. Extrinsic electromagnetic effects[15] on the optical anisotropy—due to the sample corrugations—were carefully checked.[16] Such effects are indeed present in our sample as it is not fully planarized, but they were demonstrated to yield only a shift of the overall base amplitude of the PLE signal with no effect on the peak and step positions.[16] The optical anisotropy is hence of intrinsic origin, due to the symmetry of the Bloch functions for electron and H and L holes in the valence band.[13] In-plane ([011] vs [100]) polarization anisotropy[17] has been measured on GaAs/$Al_xGa_{1-x}As$ square potential QW's grown on (011) substrates, resulting in positive (negative) anisotropy for e-H (e-L) Bloch matrix elements.[14] We calculated the anisotropy in the optical matrix elements for polarization direction along [011] ($\parallel$) and [011] ($\perp$) for the VQW's considered here, and for e-H and e-L states at BZC. The H (L) states consists of 99.15% hh (lh) and 0.85% lh (hh) components. This yields an e-H to e-L squared Bloch matrix element ratio of 0.90:0.10 for polarization along [011] and 0.01:0.99 along [011].[11] These ratios should be compared with the corresponding ones—e-hh to e-lh—for (100) QW's, i.e., 0.75:0.25 for in-plane polarization (along [011] or [011]) and 0:1 for polarization along the [100] direction, respectively. The anisotropy in optical absorption can now be explained by the above matrix elements, and in addition by the overlap of the envelope functions. The observed strong coupling of e-L (e-H) states with $\perp$ ($\parallel$) polarization results from development of hole Bloch states in a basis of spherical harmonics $|J,M_J\rangle$ with a quantization axis along the confinement direction. This is similar to (100) QW's as the $H(L)$ state in (011) QW's consists of 99% $|3/2,\pm 3/2\rangle$ ($|3/2,\pm 1/2\rangle$) states [100% for (100) QW's]. The coupling of the e_1-H_1 states in ($\perp$) polarization is, however, a specific feature of (011) QW's. It is explained by the nonvanishing (0.85%) $|3/2,\mp 1/2\rangle$ component in H states resulting from valence-band mixing of $|J,M_J\rangle$ states at BZC due to the low crystallographic symmetry in (011) QW's. The measured e_1-H_1: e_1-L_1 peak intensity ratio exceeds the corresponding calculated ratio of the overall matrix element ratio, for the ($\perp$) polarization case. This quantitative difference may be explained by the difference between absorption and PLE, the fact that dispersion and excitonic effects were not taken into account in the calculation of absorption, and that remote bands (spin-orbit, namely) have not been included in our modeling of the valence band.

Measurements of the VQW transition energies and linewidths were performed for a series of samples with $0.09 \leqslant x_{\mathrm{nom}} \leqslant 0.43$. Narrow linewidths in the order of 5 to 10 meV were obtained for the VQW transitions, which reflects the good structural uniformity of all structures for low-pressure

OMCVD growth. Comparison with the Al composition at the bottom of the VQW as measured by AFM yields an enhancement of the confinement energy with increasing x_{nom}, as the Ga segregation effect is increased and the width of the VQW branches is decreased.[4] The maximum measured Al segregation for direct interband transitions was $\Delta x = 0.16$ for $x_{\mathrm{nom}} = 0.43$, and hence yielded a total band gap energy difference of 242 meV. Polarized PLE spectra of a VQW sample with $x_{\mathrm{nom}} = 0.23$ were performed for which lateral quantum confinement effects are also evidenced.

In summary, we report direct evidence of lateral quantum confinement in VQW structures observed by PL excitation spectroscopy. It is made possible by the very good uniformity and structural definition of the multiple VQW's grown by low-pressure OMCVD. The absorption spectra show a joint density of states for interband transitions that reveals several electron and hole confined subbands. Anisotropy in the PLE spectra allows the identification of electron-to-light–holelike and electron-to-heavy–holelike transitions and is explained by valence-band mixing effects. Comparison with calculated eigenenergy levels is made possible using the Al composition profile measured by cross-sectional parallel electron energy-loss spectroscopy or atomic force microscopy across the VQW.

This work was supported in part by the Fond National Suisse de la Recherche Scientifique. The TEM and CL microscopy studies were performed at CIME-EPFL.

[1] M. Walther, E. Kapon, J. Christen, D. M. Hwang, and R. Bhat, Appl. Phys. Lett. **60**, 521 (1992).

[2] G. Vermeire, Z. Q. Yu, F. Vermaerke, L. Buydens, L. Van Daele, and P. Demeester, J. Cryst. Growth **124**, 513 (1992).

[3] W. Pan, H. Yaguchi, K. Onabe, Y. Shiraki, and R. Ito, J. Cryst. Growth **158**, 205 (1996).

[4] G. Biasiol, F. Reinhardt, A. Gustafsson, E. Martinet, and E. Kapon, Appl. Phys. Lett. **69**, 2710 (1996).

[5] A. Gustafsson, L. Samuelson, J.-O. Malm, G. Vermeire, and P. Demeester, Appl. Phys. Lett. **64**, 695 (1994).

[6] E. Kapon, B. Dwir, H. Pier, A. Gustafsson, and J.-M. Bonnard, in *Quantum Electronics and Laser Science Conference* (OSA, Baltimore, 1995).

[7] V. Berger, G. Vermeire, P. Demeester, and C. Weisbuch, Appl. Phys. Lett. **66**, 218 (1995).

[8] X.-L. Wang, M. Ogura, and H. Matsuhata, Appl. Phys. Lett. **67**, 804 (1995).

[9] N. Usami, W. Pan, H. Yaguchi, R. Ito, K. Onabe, H. Akiyama, and Y. Shiraki, Appl. Phys. Lett. **68**, 3221 (1996).

[10] K. Leifer, Ph.D. thesis, EPFL, 1997; K. Leifer and P. A. Buffat, Inst. Phys. Conf. Ser. (to be published).

[11] E. Martinet (unpublished).

[12] C. Bosio, J. L. Staehli, M. Guzzi, G. Burri, and R. A. Logan, Phys. Rev. B **38**, 3263 (1988).

[13] Y. Kajikawa, M. Hata, and T. Isu, Jpn. J. Appl. Phys. **30**, 1944 (1991).

[14] Y. Kajikawa, M. Hata, T. Isu, and Y. Katayama, Surf. Sci. **267**, 501 (1992).

[15] U. Bockelmann, Europhys. Lett. **16**, 601 (1991).

[16] F. Vouilloz, D. Y. Oberli, M. A. Dupertuis, A. Gustafsson, F. Reinhardt, and E. Kapon, Phys. Rev. Lett. **78**, 1580 (1997).

[17] The in-plane anisotropy is defined from the squared Bloch matrix elements (M) in the different polarizations, as $(M^2_{[011]} - M^2_{[100]})/(M^2_{[011]} + M^2_{[100]})$.